

# The X-ray Properties of M101 ULX-1= CXOKM101 J140332.74+542102

K. Mukai<sup>1</sup>, M. Still<sup>1</sup>, R.H.D. Corbet<sup>1</sup>

*Exploration of the Universe Division, Code 662, NASA/Goddard Space Flight Center,  
Greenbelt, MD 20771*

mukai@milkyway.gsfc.nasa.gov

K.D. Kuntz

*Henry A. Rowland Department of Physics and Astronomy, Johns Hopkins University,  
Homewood Campus, Baltimore, MD 21218, and Exploration of the Universe Division, Code  
662, NASA/Goddard Space Flight Center, Greenbelt, MD 20771*

and

R. Barnard

*Department of Physics and Astronomy, The Open University Walton Hall, Milton Keynes  
MK7 6BT, UK*

## ABSTRACT

We report our analysis of X-ray data on M101 ULX-1, concentrating on high state *Chandra* and *XMM-Newton* observations. We find that the high state of M101 ULX-1 may have a preferred recurrence timescale. If so, the underlying clock may have periods around 160 or 190 days, or possibly around 45 days. Its short-term variations resemble those of X-ray binaries at high accretion rate. If this analogy is correct, we infer that the accretor is a 20–40  $M_{\odot}$  object. This is consistent with our spectral analysis of the high state spectra of M101 ULX-1, from which we find no evidence for an extreme ( $> 10^{40}$  ergs s<sup>-1</sup>) luminosity. We present our interpretation in the framework of a high mass X-ray binary system consisting of a B supergiant mass donor and a large stellar-mass black hole.

*Subject headings:* X-rays: individual (M101 ULX-1) — X-rays: binaries

---

<sup>1</sup>Also Universities Space Research Association

## 1. Introduction

It is now clear that some X-ray sources in external galaxies are brighter than those seen in our Galaxy, thus providing a strong scientific motivation for high spatial resolution X-ray studies. Off-nuclear sources in nearby galaxies with luminosities exceeding  $10^{39}$  ergs s<sup>-1</sup> have been designated ultraluminous X-ray sources (ULXs). The nature of ULXs, in particular whether they are powered by intermediate-mass black holes (IMBH,  $M > 100 M_{\odot}$ ) that are distinct from stellar-mass and supermassive black holes, has become a hotly debated issue (Fabbiano 2005). If their X-ray emissions are isotropic and sub-Eddington, the compact objects in ULXs must be at least 7 solar masses ( $7M_{\odot}$ ).

Our object of study here is CXOKM101 J140332.74+542102 (hereafter M101 ULX-1), a highly variable source in the nearby (7.2 Mpc; Stetson et al. 1998) face-on spiral galaxy, M101, whose ULX phase was discovered in the 2000 March *Chandra* observations (Pence et al. 2001; Mukai et al. 2003). Kuntz et al. (2005) have discovered an optical counterpart of M101 ULX-1, with brightness and colors consistent with those of a B supergiant in M101, hence it is almost certainly a high-mass X-ray binary (HMXB). Also throughout 2004, we carried out a series of *Chandra* observations totaling a million seconds of exposure time (hereafter “Msec”) for a comprehensive X-ray study of M101, including monitoring of bright individual sources. Kong et al. (2004) have analyzed a subset of these data and claim that M101 ULX-1 reached a peak 0.3–7 keV luminosity of  $3 \times 10^{40}$  ergs s<sup>-1</sup> in July 2004, a claim which we reexamine in §3.3, after considering the long-term and short-term variability in §3.1 and §3.2, respectively. We then reassess the nature of M101 ULX-1 in §4.

## 2. Observations

The Msec data set, as well as our reduction method, will be described fully in Kuntz (2005). In addition, we have analyzed all archival *ROSAT*, *Chandra*, and *XMM-Newton* observations of M101 to establish the long-term history of M101 ULX-1. Here we present our detailed analysis of the high state *Chandra* and *XMM-Newton* data. The relevant datasets are summarized in Table 1. We do not analyze the low state data in detail; any effort to analyze them (e.g., Kong et al. 2004) is necessarily limited by the poor statistics. In addition, there is potential for source confusion in a low state, since we cannot rule out a faint contaminating source at luminosities up to  $10^{36}$  ergs s<sup>-1</sup>.

### 3. Analysis

#### 3.1. Long-term Variability

We have reconstructed the long-term light curve of M101 ULX-1. We compute the 0.3–2.5 keV luminosity using an absorbed blackbody plus power law model for the high signal-to-noise data (all data marked as “high state” in Table 1 as well as the 2000 October *Chandra* and 2004 July *XMM-Newton* observations). For fainter data, we convert from count rates to luminosity using a conversion factor derived from 2004 July *XMM-Newton* data. We similarly estimate the luminosity during earlier *ROSAT* observations. We present the resulting light curve in Figure 1, once for the entire period (1991 June through 2005 January) and once for the *Chandra-XMM-Newton* era (2000 March through 2005 January). The most obvious feature of this is the recurrent high states. We investigate if there is an underlying periodicity in these high states.

High states of M101 ULX-1 appear to have durations of over eighteen days, though the amount of time spent at the peak luminosity is significantly shorter, judging from the lightcurves of the 2004 July and 2004 December/2005 January high states. The intervals between the 2000 March high state and the 2000 October high state (216 days) and that between the 2004 July high state and the 2004 December/2005 January high state (151 days) are incommensurate, implying that the high states of M101 ULX-1 does not repeat on a strict period.

In order to explore the characteristic time scales of the system, we have classified each observation as either “high” ( $L_X > 10^{37.5}$  ergs s<sup>-1</sup>) or “low.” We attempted to match this bimodal light-curve with a square wave with period  $P$ , phase, and an activity fraction as free parameters. If the source were strictly periodic, then the activity fraction would correspond to the duty fraction. For a source that is not strictly periodic, the activity fraction corresponds to the width of a “window” in which the source is likely to be active, convolved with the duty fraction.

We have explored three different data selections: The well sampled interval from 2004 January to 2005 January (the Msec interval), the less well sampled interval from 2000 March to 2005 January (the *ChandraXMM-Newton* era), and the entire interval, which includes the *ROSAT* data as well. These selections allow us to investigate a range of periods, allowing for departures from a strict periodicity.

We have tested periods from 20 to 250 days, and activity fractions from 1% to 60%. Figure 2 (left) shows the regions with the best matches to the data for the three different data selections. Note that, given the high/low simplification of the light curve used in our

analysis, the regions in this plot are either allowed or not allowed, with no quantitative goodness of fit in the usual sense. The Msec epoch data allow “periods” of 154–163 days and 187–199 days, with no data-model mismatches. The more extended interval does not allow a solution if we require that all data points match the model. However, if we allow one mismatch, periods of 159 days and 189–199 days are allowed. The entire dataset has a periodic solution only if we allow two observations to be mismatched. “Periods” with only two mismatches are 156 days, 159 days, 172–174 days, and 193–197 days. Thus, no matter which data subset was chosen, “periods” around 159 and 195 days best matched the data, but the longer the interval, the more mismatches are required.

We also investigated if a shorter period ( $<60$  days) might match the data (Figure 2 right). Using the Msec interval, the best solutions (45 days) would produce two mismatches, usually the 2004 July *XMM-Newton* observation, and either the first or last observations of an extended set of *Chandra* observations. Longer fit intervals produced greater numbers of mismatches for their best fits.

This analysis suggests that M101 ULX-1 has a characteristic time-scale. It is not a strict periodicity, although it is still possible that it is a superposition of periodic and random variations.

### 3.2. Short-term Variability

We present the light curves of 2004 July and 2004 December/2005 January high states in Figure 3 and Figure 4, respectively. The high degree of short-timescale variability is obvious. Moreover, we confirm our earlier results (Mukai et al. 2003) of the energy dependence of the variability: M101 ULX-1 is more variable at higher energies.

The power density spectra (PDS) of disk-accreting X-ray binaries can be classified into two broad categories based on whether the Eddington accretion rate ( $l=L/L_{\text{Edd}}$ ) is above or below the critical value,  $l_c$ , regardless of the nature of the primary (van der Klis 1994). At low accretion rate ( $l < l_c$ ), X-ray binaries have a fractional rms amplitude of a few times 10% and a broken power law PDS (hereafter Type A); at high accretion rate ( $l > l_c$ ), they have a fractional rms of a few percent, with power law (index 1–1.5) PDS (Type B). Although there is a well-known hysteresis effect (Miyamoto et al. 1995) that complicates the situation, Barnard et al. (2004) have nevertheless obtained an empirical calibration of  $l_c$  of 0.1, in terms of observed 0.3–10 keV luminosity as a fraction of the Eddington limit. They (see also Barnard et al. 2003) have applied this to identify black hole candidates in M31.

We have performed a similar PDS analysis of M101 ULX-1, both from the 2000 March

observation and from the 2004 July observations (Figure 5). The PDSs can be described by a power law with a slope of about  $-1$ , merging into the photon counting noise at  $10^{-3}$  Hz. This is consistent with a Type B PDS for an extragalactic X-ray binary, implying that the Eddington accretion rate of the source was in the range 0.1–1.0 both in 2000 March and in 2004 July. Therefore, equating our estimate of the 0.3–10 keV luminosity in 2004 July of  $\sim 6 \times 10^{38}$  ergs s $^{-1}$  (§3.3) with  $0.1 L_{\text{Edd}}$ , we infer the upper limit of compact object mass of  $\sim 40 M_{\odot}$ . If the X-rays we observe from M101 ULX-1 are beamed, then the true luminosity is lower, and the compact object mass is also lower. On the other hand, equating the highest luminosity we measure ( $3 \times 10^{39}$  ergs s $^{-1}$ ) with  $L_{\text{Edd}}$ , we infer a lower limit of  $20 M_{\odot}$ , again assuming that there is no beaming and M101 ULX-1 stays sub-Eddington at all times. However, the latter assumption need not apply strictly, since it is quite possible for an accreting object to exceed its Eddington limit for a short time.

### 3.3. High State Spectra

We have investigated the high state spectra of M101 ULX-1, first using an absorbed blackbody model (Mukai et al. 2003; Kong et al. 2004). When applied to the 2004 July data, we obtain an high absorbing column ( $N_{\text{H}} \sim 2 \times 10^{21}$  cm $^{-2}$ ) and an absorbed 0.3–7 keV luminosity of  $\sim 4 \times 10^{38}$  ergs s $^{-1}$ . (Note that the  $3 \times 10^{40}$  ergs s $^{-1}$  value claimed by Kong et al. (2004) is the unabsorbed luminosity in the 0.3–7 keV band).

The X-ray absorbing column inferred by this fit is well above the Galactic column of  $\sim 10^{20}$  cm $^{-2}$  and the total absorption through the disk of M101 ( $\sim 6 \times 10^{20}$  cm $^{-2}$ ). If this X-ray column was due to normal interstellar matter, this translates to an expected color excess  $E_{B-V}$  of  $\sim 0.33$  (Bohlin et al. 1978), or a visual extinction  $A_V$  of  $\sim 1$  magnitude. In contrast, the optical counterpart has a  $B-V$  color of  $-0.15 \pm 0.12$ , which is consistent with that of a B supergiant with little reddening (see Figure 4 of Kuntz et al. 2005). In fact, an assumed value of  $A_V = 0.4$  will make the optical counterpart intrinsically bluer than any early type stars. Moreover, there is a suggestion of day-to-day variability of  $N_{\text{H}}$  during the interval July 5–12, 2004 in the spectral fits by Kong et al. (2004). Therefore, if this model is correct, a significant fraction of the X-ray absorber is likely to be located within the binary or in its immediate surroundings and is thus subject to an intense ionizing radiation.

Given this, we have also fitted the average (July 5–11) spectrum using a blackbody plus ionized absorber model (the latter implemented in XSPEC as “absori”). Highly ionized matter is essentially transparent at soft X-ray energies, and even a small ( $\xi = 1$ ) ionization makes the fit visibly worse (Figure 6; Table 2). We therefore conclude that the observed shape of the soft X-ray spectrum demands a near neutral absorber, if a blackbody (or a

disk blackbody) is the intrinsic spectrum shape. What if the intrinsic spectral shape is a blackbody with absorption edges in the *Chandra* band, as Kong et al. (2004) claimed? We can indeed fit the 2004 July spectrum with modest interstellar column ( $4 \times 10^{20} \text{ cm}^{-2}$ ), but only if we include a strong edge below the ACIS band, e.g., at 0.28 keV. We show one such example in Figure 6, resulting in a 63 eV blackbody with edges at 0.28 and 0.56 keV. However, a strong edge below 0.3 keV requires low Z elements (presumably C) with K-shell electrons. That is, such an edge is in fact the sign of a near neutral absorber. We therefore conclude that the presence of a neutral absorber is required to explain the observed curvature of the spectrum below  $\sim 0.5$  keV.

We have then analyzed all high state spectra obtained with *Chandra* together. These are the 2000 March observation analyzed by Mukai et al. (2003); the 2004 July observations; and the 2004 December/2005 January observations. We omit the 2000 October observation, since M101 ULX-1 was relatively faint, although still well within the high state, and the exposure time was short ( $< 10$  ksec). We re-use the subdivision of 2000 March data into high, medium, and low intensity states as defined by Mukai et al. (2003). When M101 ULX-1 is at its brightest, we observe an excess of counts above 2 keV, which can be fitted with an additional power law. However, the parameters of this component is poorly constrained, so we concentrate on fitting below 2 keV.

Using the blackbody model absorbed only with a neutral absorber, we plot the blackbody temperature, the absorbing column, and the inferred bolometric luminosity against the count rates in the left column of Figure 7. We use the observed count rates for the Msec observations, but scale the 2000 March count rates by the ratio of 0.3–1 keV effective areas to approximately account for the loss of low energy response in ACIS-S.

We immediately see that both  $N_H$  and the inferred bolometric luminosity ( $L_{\text{bol}}$ ) have a negative correlation with the observed count rate. The similarity of behavior of the two suggests there is a common origin. We propose that this is an artifact of the absorbed blackbody fit: if the true spectrum of M101 ULX-1 is more strongly peaked than a blackbody, blackbody fits will be forced to a high  $N_H$  value and inflate the inferred  $L_{\text{bol}}$ .

To test this hypothesis, we have fitted these 6 spectra with a second model. After some experimentation, we have fixed  $N_H$  to  $4 \times 10^{20} \text{ cm}^{-2}$ , a reasonable value for an object in the disk of M101. The underlying model is a variable blackbody plus a relativistic line from an accretion disk (“diskline” as implemented in *xspec*)<sup>1</sup>. This model is often invoked for the Fe

---

<sup>1</sup>A simple Gaussian line is a valid alternative. However, the asymmetric shape of the “diskline” profile with sharp drop of the blue wing and a more gradual drop of the red wing gives a somewhat better fit for some of the spectra.

K lines in active galactic nuclei (AGN). More recently, Branduardi-Raymont et al. (2001) have fitted the *XMM-Newton* RGS spectra of two AGN using relativistic lines from OVIII, NVI, and CV, and the same physical interpretation can in principle apply to M101 ULX-1.

The parameters for the diskline were fixed at the following values, after experimentation: the central energy, 0.5 keV;  $\beta$  (power law index for the radial dependence of emissivity),  $-2$ ; range of accretion disk radius, 6–1000  $M_g$ ; and disk inclination,  $75^\circ$ . We show the July 2004 data as fitted with this model in Figure 6. The line energy (0.5 keV) suggests NVI, while for this spectrum alone (in fact, only the July 6 spectrum), an additional line at 0.8 keV would further improve the fit. Alternatively, this feature could be due to a transient edge at 0.9 keV (Kong et al. 2004). As for the 0.6 keV edge also noted by Kong et al. (2004), this is not required for a good fit once the 0.5 keV emission line is included in the model.

We summarize the results for all high state spectra in Table 3 and in the right column of Figure 7. In contrast to the absorbed blackbody fits, the inferred  $L_{\text{bol}}$  values are positively correlated with the count rates using this model. The inferred bolometric luminosity and the unabsorbed 0.3–10 keV luminosity for the 2004 July data are  $\sim 1 \times 10^{39}$  ergs  $\text{s}^{-1}$  and  $\sim 6 \times 10^{38}$  ergs  $\text{s}^{-1}$ , in contrast to the much higher value obtained with the absorbed blackbody fit. The 2005 January *XMM-Newton* data can also be fitted with either model (Table 3). In these fits, the model parameters are statistically well-constrained (e.g., the blackbody temperature has typical errors of 5 to 20 eV), but it is clear that the true uncertainties are dominated by the systematics due to our choice of models.

## 4. Discussion

### 4.1. Nomenclature

Various authors have borrowed existing terminology to describe M101 ULX-1 and other bright X-ray sources in nearby galaxies. On closer inspection, however, the applied terminology often fails to meet the traditional definition used in the Galactic X-ray Binary community. We have therefore considered, and ultimately declined to use, two nomenclatures that have been applied to M101 ULX-1.

Super-soft sources (SSSs) are luminous soft X-ray sources with equivalent blackbody temperatures of  $\sim 15$ – $80$  eV and estimated bolometric luminosities of  $10^{36}$ – $10^{38}$  ergs  $\text{s}^{-1}$  (Kahabka & van den Heuvel 1997). It is generally accepted that, with few exceptions, SSSs are nuclear burning white dwarfs. However, some authors (see, e.g., Di Stefano & Kong 2003) have sought to expand the definition of the class in recent years. While the expanded definition allows these authors to draw attention to a collection of interesting objects, they are

likely to be a heterogeneous mixture. We prefer to preserve the well-established connotation of SSS with nuclear burning white dwarfs. Pence et al. (2001) identified 10 *Chandra* sources in M101 as supersoft, using a hardness ratio criterion that approximates the traditional definition: these sources have no counts above 0.8 keV. On the other hand, M101 ULX-1 was in a high state at the time and had significant counts even above 1.3 keV. We therefore do not consider M101 ULX-1 to be an SSS.

The other terminology we discuss is “X-ray transient,” for which it is difficult to find a formal definition. Historically, this term is applied to Galactic X-ray sources that are detectable by all-sky monitors at one epoch and undetectable in pointed observations using collimated (non-imaging) instruments. In particular, soft X-ray transients, which are believed to be due to disk instability (Lasota 2001), usually have quiescent luminosity less than  $10^{34}$  ergs s<sup>-1</sup>. With the current generation of instruments, sources in M101 that are fainter than  $10^{36}$  ergs s<sup>-1</sup> are undetectable in a single observation. Such an upper limit is far too high to establish the presence of a true transient, although it is certainly possible to find candidate transients (Jenkins et al. 2005). In the specific case of M101 ULX-1, it is unknown if it ever becomes fainter than  $10^{36}$  ergs s<sup>-1</sup>. For this reason, we have not used the term “transient” to describe M101 ULX-1, nor have we used the related terms “quiescent” and “outburst,” instead preferring the more neutral terms, “high state” and “low state.”

## 4.2. The Nature of the Compact Object

Kong et al. (2004) have analyzed the 2004 July spectra of M101 ULX-1 using the absorbed blackbody model, inferred a bolometric luminosity of  $\sim 10^{41}$  ergs s<sup>-1</sup>, and concluded that M101 ULX-1 must contain an IMBH. Using the Eddington luminosity argument,  $\sim 10^{41}$  ergs s<sup>-1</sup> corresponds to a minimum mass of 700  $M_{\odot}$ . However, our spectral analysis above makes it clear that this conclusion is highly model-dependent. We argue, moreover, that the absorbed blackbody fits have two shortcomings: the requirement for a neutral absorber next to a  $>10^{40}$  ergs s<sup>-1</sup> X-ray source, and the counterintuitive trend of fitted parameters against *Chandra* count rate.

As noted earlier, the high and variable values of the X-ray absorber in the absorbed blackbody fits (Figure 7) require the absorber to be in the vicinity of M101 ULX-1 itself. Whereas the presence of such intra- or circum-binary material is expected, due to the copious mass loss from the supergiant mass donor, it is likely to be highly ionized on average (see, e.g., Wojdowski et al. 2000), even when the luminosity is a few times  $10^{38}$  ergs s<sup>-1</sup>; much more so if the bolometric luminosity is near  $10^{41}$  ergs s<sup>-1</sup>. While high density clumps with lower than average ionization are expected, we need extreme clumping to explain the observed



absorber. For example, for a clump  $10^{13}$  cm from a  $10^{41}$  ergs $s^{-1}$  source to have  $\xi < 1$ , a density greater than  $10^{15}$  cm $^{-3}$  is required; for such a clump to be responsible for the observed X-ray absorption of  $N_{\text{H}} \sim 2 \times 10^{21}$  cm $^{-2}$ , it must have a length of only  $\sim 2 \times 10^6$  cm. A clump at a distance of  $10^{15}$  cm needs a density  $> 10^{11}$  cm $^{-3}$  and a length of  $\sim 2 \times 10^{10}$  cm. That is, for such a clump to remain neutral, it must have a high overdensity factor, and hence a small filling factor. We therefore consider the inferred neutrality of the X-ray absorber to be a severe problem for the absorbed blackbody interpretation.

This model also leads to a counterintuitive trend with observed count rate (Figure 7; Table 3), whereas our alternative spectral model does not suffer from this problem. We do not necessarily claim that our model is the correct physical description of M101 ULX-1. Nevertheless, it is comforting to note that a simple analytical model, with a physical interpretation (relativistic emission line from the accretion disk) can fit the collection of high state spectra without requiring an anti-correlation between observed count rate and bolometric luminosity, or the presence of a neutral absorber within an ULX system. It is quite possible that other models can be found that can fit the available data equally well. Any model that fits the data without requiring a high  $N_{\text{H}}$  will likely result in a moderate bolometric luminosity in 2004 July of  $\sim 1 \times 10^{39}$  ergs $s^{-1}$ .

We conclude that there is no compelling evidence for an IMBH of the sort claimed by Kong et al. (2004) ( $\gg 100 M_{\odot}$ ) in M101 ULX-1. We furthermore consider that the accreting object is likely a 20–40  $M_{\odot}$  black hole from our PDS analysis (§3.2). The X-ray spectrum of M101 ULX-1 is unlike those of well-established stellar-mass black hole candidates, but this is common problem for all models of M101 ULX-1. Before proceeding further with this interpretation, we briefly consider possible alternatives.

Can M101 ULX-1 contain a nuclear burning white dwarf, given that the high state spectrum of M101 ULX-1 is dominated by a soft, blackbody-like component? There is indeed a superficial similarity between M101 ULX-1 and SSS. However, M101 ULX-1 is too hot at times (kT as high as 0.2 keV), and the observed luminosity in 2000 March (before absorption and bolometric corrections) is well above the Eddington limit for a white dwarf. High luminosity is thought to drive a strong (but non-relativistic) outflow, expanding the white dwarf photosphere and driving the emission to longer wavelength (see, e.g., Kato 1997). Beaming is unlikely, since the supersoft emission in a nuclear burning white dwarf is photospheric, and no relativistic jet is expected. Thus, a white dwarf accretor appears unlikely in this case.

Can it be a neutron star? Many X-ray pulsars have a soft component often modeled as a blackbody with kT $\sim$ 0.1 keV (Hickox et al. 2004), which is also pulsed. If it is a pulsar, its emission is by definition beamed, so the Eddington luminosity argument loses its punch.

Although accreting pulsars are usually dominated by a hard power-law component in the *Chandra* band, different beaming of the hard and soft component might make M101 ULX-1 appear dominated by the soft component. Our timing analysis is limited by the time resolution of the ACIS data in the high state and the lack of photons in the low state, so a  $P_{spin} \sim 1$ s pulsar would have not been detected. This possibility should be kept in mind for M101 ULX-1, but does require a factor of 10 beaming of the soft component to explain the highest luminosity data.

### 4.3. The Nature of the Binary System

We therefore return to the interpretation we consider most likely, that M101 ULX-1 is a high-mass X-ray binary (HMXB) with a B supergiant mass donor (Kuntz et al. 2005) and a 20–40  $M_{\odot}$  black hole. At the low end of our preferred range, it can be considered a normal stellar-mass black hole, while at the high end, it is more massive than those predicted by the standard theory of stellar evolution. It is unclear, however, if a radically different formation mechanism is required for such a black hole. In any case, the binary as a whole shows a family resemblance to the more familiar HMXBs.

One well-known system to which M101 ULX-1 might be compared is Cyg X-1, for which the transitions to and from the low/hard state and the high/soft state enhance the apparent variability, depending on the bandpass of the X-ray instrument. Its count rates varies by a factor of  $\sim 10$  in the *RXTE* ASM, which is sensitive to 2–10 keV X-rays. With the exception of the orbital period, there is no known periodic component in its long-term light curves, even though there are well-studied correlations between average brightness, X-ray spectral shape, X-ray PDS, and the radio emission (Gleissner et al. 2004a,b). We might simply consider M101 ULX-1 to be an extreme cousin of Cyg X-1, perhaps related to the higher black hole mass.

Alternatively, the long-term modulation of M101 ULX-1 may be a “super-orbital” variability seen in several Galactic and Magellanic X-ray binaries (see, e.g., Clarkson et al. 2004). Radiation-induced warping of the accretion disk is the leading candidate mechanism for such modulations; it typically operates in high-luminosity, Roche-lobe overflow systems and the resultant modulations are not strictly periodic.

The long-term light curve suggests that M101 ULX-1 is usually in a low state, with secular average luminosity of about  $10^{37}$  ergs  $s^{-1}$ . For a black hole with accretion efficiency ( $L/\dot{m}c^2$ ) of 10%, an accretion rate of  $1.1 \times 10^{17}$  g  $s^{-1}$  or  $1.8 \times 10^{-9}$   $M_{\odot}$   $yr^{-1}$  is required to produce  $10^{37}$  ergs  $s^{-1}$ . It is possible to achieve such an accretion rate through wind accretion,

without the mass donor filling its Roche lobe. If so, the long-term variation may reflect the orbital period of an eccentric binary. For example, GX301–2 is a 41.5 day period, eccentric ( $e=0.462$ ) binary in which a neutron star accretes the wind of a supergiant mass donor (see, e.g., Kreykenbohm et al. 2004). The analogy would be very close if the long-term modulation is an irregular manifestation of an underlying 45-day clock (Figure 2 right).

In conclusion, the observations so far of M101 ULX-1 are consistent with this being a high mass X-ray binary with a B supergiant mass donor and a large stellar mass black hole. The long-term variability may have an underlying periodic clock, and this should be investigated with further X-ray observations. At the same time, ground-based optical spectroscopy should be pursued in search of the orbital period.

## REFERENCES

- Barnard, R., Osborne, J.P., Kolb, U. & Borozdin, K.N. 2003, *A&A*, 405, 505
- Barnard, R., Kolb, U. & Osborne, J.P. 2004, *A&A*, 423, 147
- Bohlin, R.C., Savage, B.D. & Drake, J.F. 1978, *ApJ*, 224, 132
- Branduardi-Raymont, G., Sako, M., Kahn, S.M., Brinkman, A.C., Kaastra, J.S. & Page, M. 2001, *A&A*, 365, L140
- Clarkson, W.I., Charles, P.A., Coe, M.J. & Laycock, S. 2004, *MNRAS*, 343, 1213
- Di Stefano, R. & Kong, A.K.H. 2003, *ApJ* 592, 884
- Di Stefano, R. & Kong, A.K.H. 2004, *ApJ* 609, 710
- Di Stefano, R., Kong, A.K.H., Greiner, J., Primini, F.A., Garcia, M.R., Barmby, P., Massey, P., Hodge, P.W., Williams, B.F., Murray, S.S., Curry, S. & Russo, T.A. 2004, *ApJ*, 610, 247
- Fabbiano, G. 2005, *Science*, 307, 533.
- Gleissner, T., Wilms, J., Pottschmidt, K., Uttley, P., Nowak, M.A. & Staubert, R. 2004, *A&A*, 414, 1091
- Gleissner, T., Wilms, J., Pooley, G.G., Nowak, M.A., Pottschmidt, K., Markoff, S., Heinz, S. Klein-Wolt, M., Fender, R.P. & Staubert, R. 2004, *A&A*, 425, 1061
- Hickox, R.C., Narayan, R. & Kallman, T.R. 2004, *ApJ* 614, 881
- Jenkins, L.P., Roberts, T.P., Warwick, R.S., Kilgard, R.E. & Ward, M.J. 2005, *MNRAS* 357, 401
- Kahabka, P. & van den Heuvel, E.P.J. 1997, *Ann. Rev. A. Ap.* 33, 69
- Kato, M. 1997, *ApJS*, 113, 121
- Kong, A.K.H., Di Stefano, R. & Yuan, F. 2004, *ApJ*, 617, L49
- Kreykenbohm, I., Wilms, J., Coburn, W., Kuster, M., Rothschild, R.E., Heindl, W.A., Kretschmar, P. & Staubert, R. 2004, *A&A*, 427, 975
- Kuntz, K.D. 2005, *ApJ*, in preparation

- Kuntz, K.D., Gruendl, R.A., Chu, Y.-H., Chen, C.-H. R., Still, M., Mukai, K. & Mushotzky, R.F. 2005, ApJ, 620, L31
- Lasota, J.-P. 2001, NewAR, 45, 449
- Leahy, D.A., Darbro, W., Elsner, R.F., Weisskopf, M.C., Kahn, S., Sutherland, P.G. & Grindlay, J.E. 1983, ApJ, 266, 160
- Miyamoto, S., Kitamoto, S., Hayashida, K. & Egoshi, W. 1995, ApJ, 442, L13
- Mukai, K., Pence, W.D., Snowden, S.L. Kuntz, K.D. 2003, ApJ, 582, 184
- Pence, W.D., Snowden, S.L., Mukai, K. & Kuntz, K.D. 2001, ApJ, 561, 189
- Stetson, P.B., et al. 1998, ApJ 508, 491
- van der Klis, M. 1994, ApJS, 92, 511
- Wojdowski, P.S., Clark, G.W. & Kallman, T.R. 2000, ApJ 541, 963

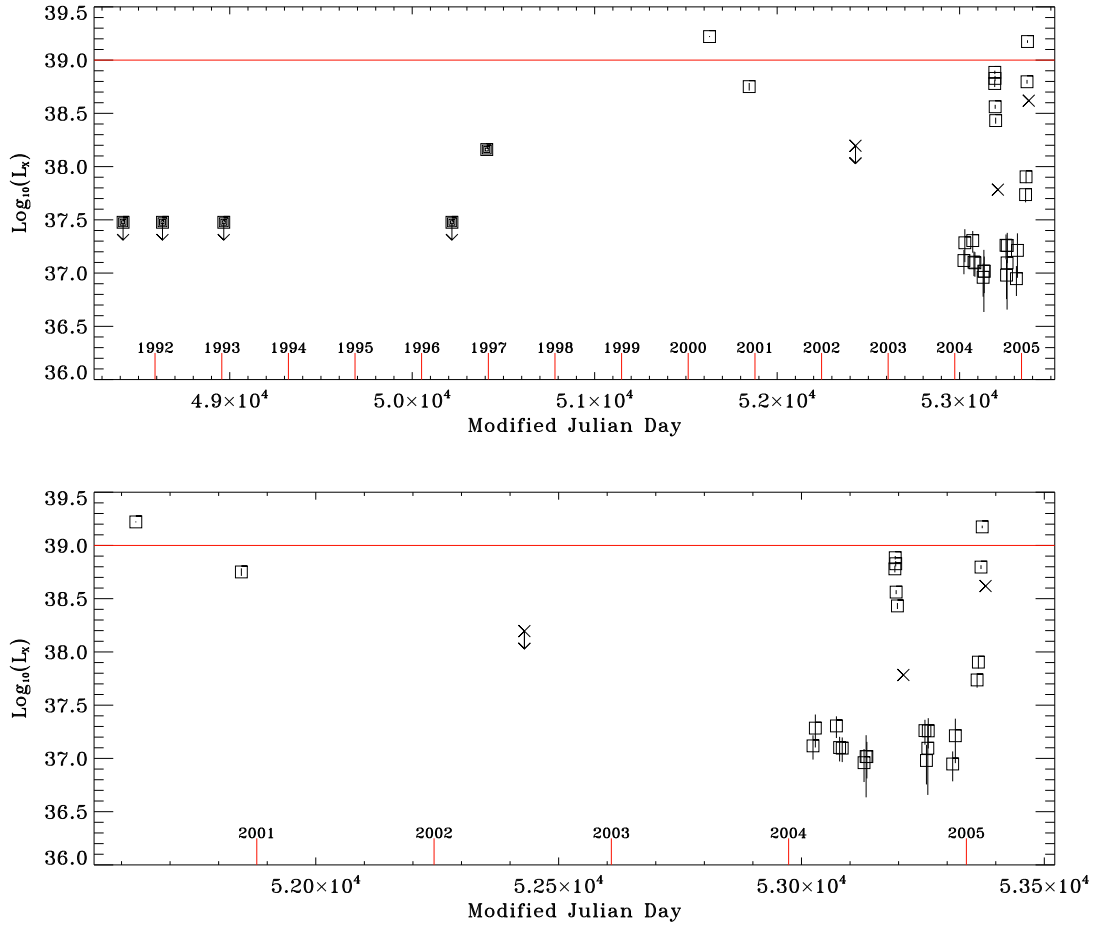


Fig. 1.— The long-term light curve (0.3–2.5 keV luminosity) of M101 ULX-1 from *ROSAT* (filled square), *Chandra* (open square), and *XMM-Newton* (cross) data, in two panels. The upper panel shows the light curve over the period 1991–2005, while the lower panel shows a blow up for the period 2001–2005.

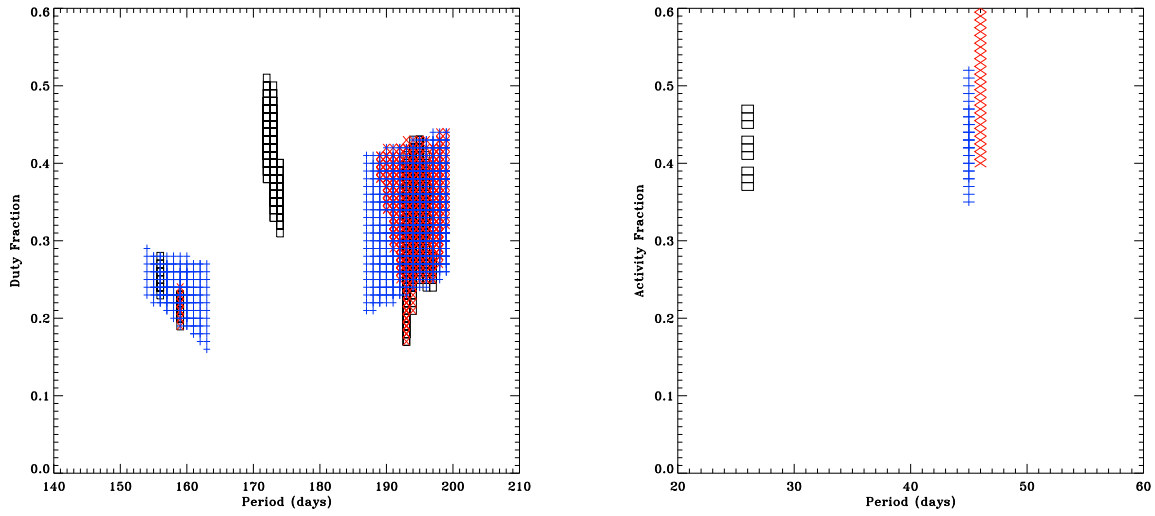


Fig. 2.— **Left:** The region of the period-activity space with the best match to the data using the Msec interval (*Crosses* no mismatches), the Chandra-XMM era interval (*Xs* one mismatch), and the entire interval (*Squares* two mismatches). **Right:** The short-period region of the period-activity space with the best match to the data using the Msec interval (*Crosses* two mismatches), the Chandra-XMM era interval (*Xs* three mismatch), and the entire interval (*Squares* four mismatches).

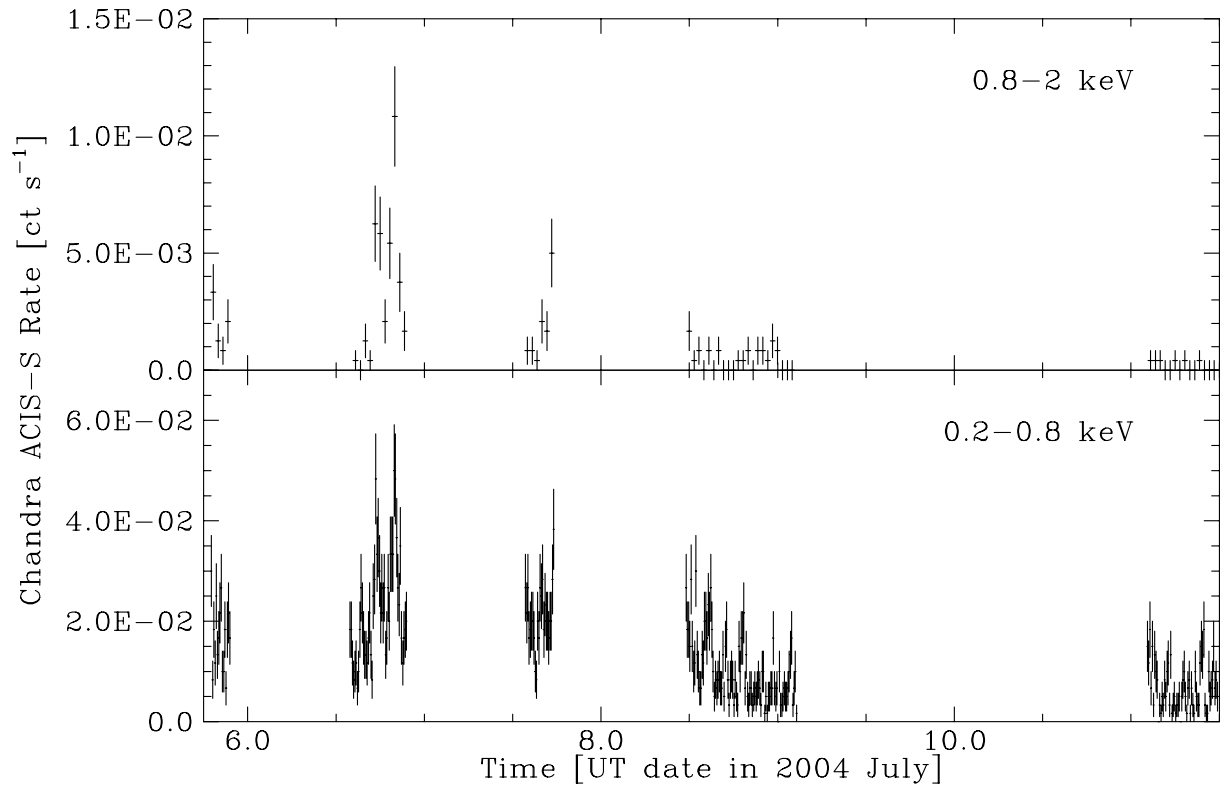


Fig. 3.— *Chandra* ACIS-S light curve of M101 ULX-1 in 2004 July in two bands; one bin is 600s for the 0.2–0.8 keV band and 2400s for the 0.8–2 keV band.



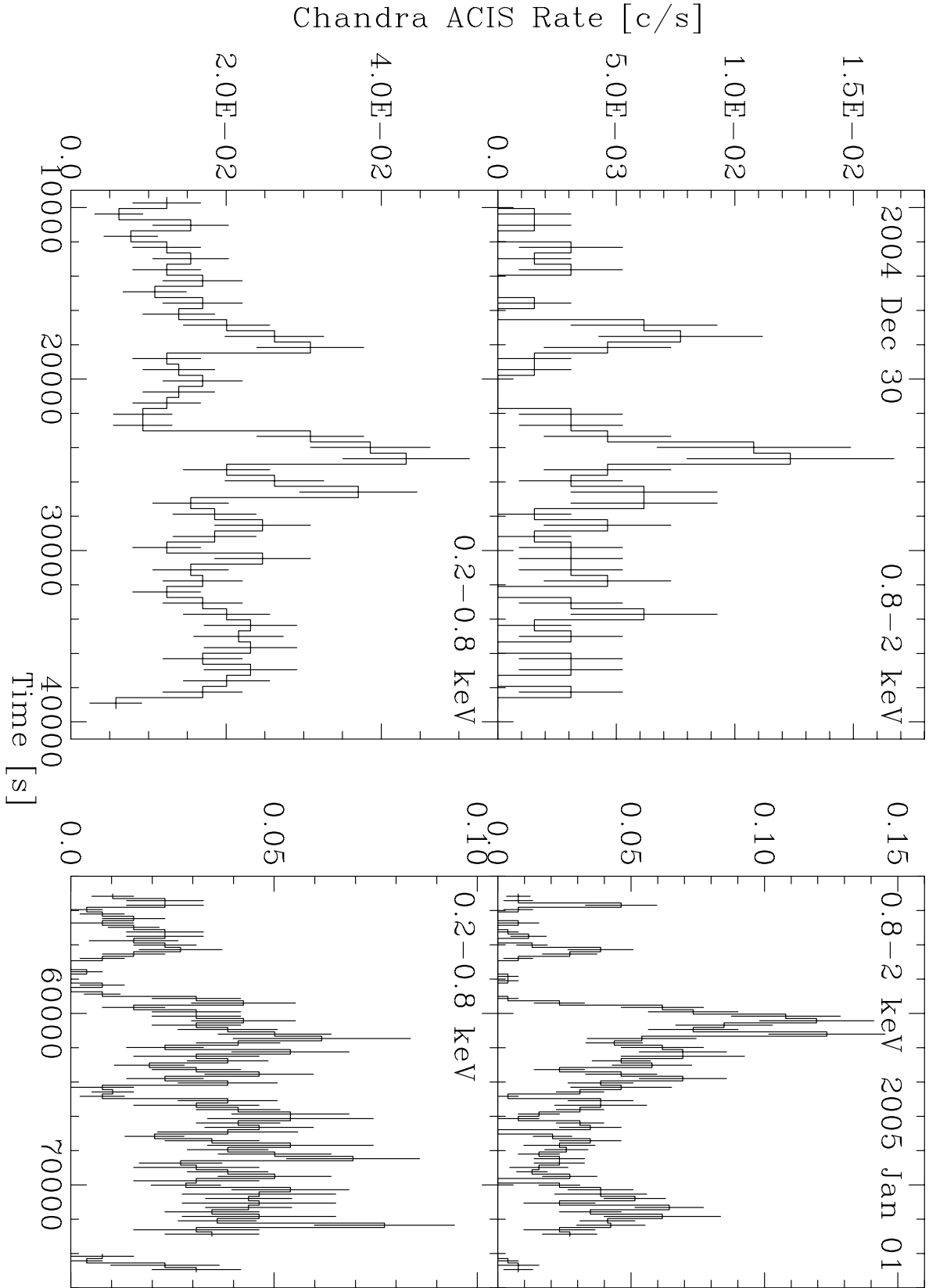


Fig. 4.— *Chandra* ACIS-S light curve of M101 ULX-1 on 2004 December 30 (in 648 s bins) and on 2005 January 1 (256 s bins), in two energy bins.

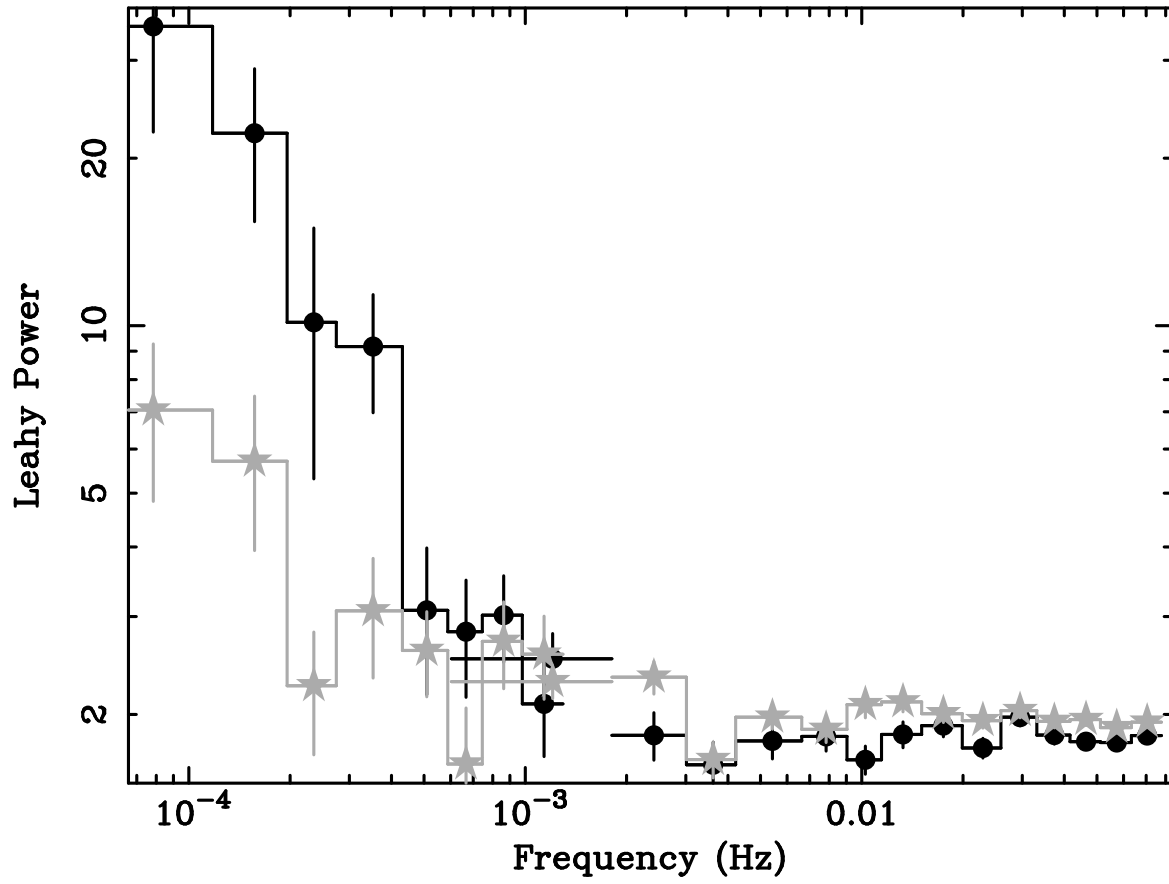


Fig. 5.— Power Density Spectrum of M101 ULX-1 in 2000 March (black) and 2004 July (grey), normalized according to the prescription of Leahy et al. (1983) so that the expected Poisson noise results in a mean power of 2.

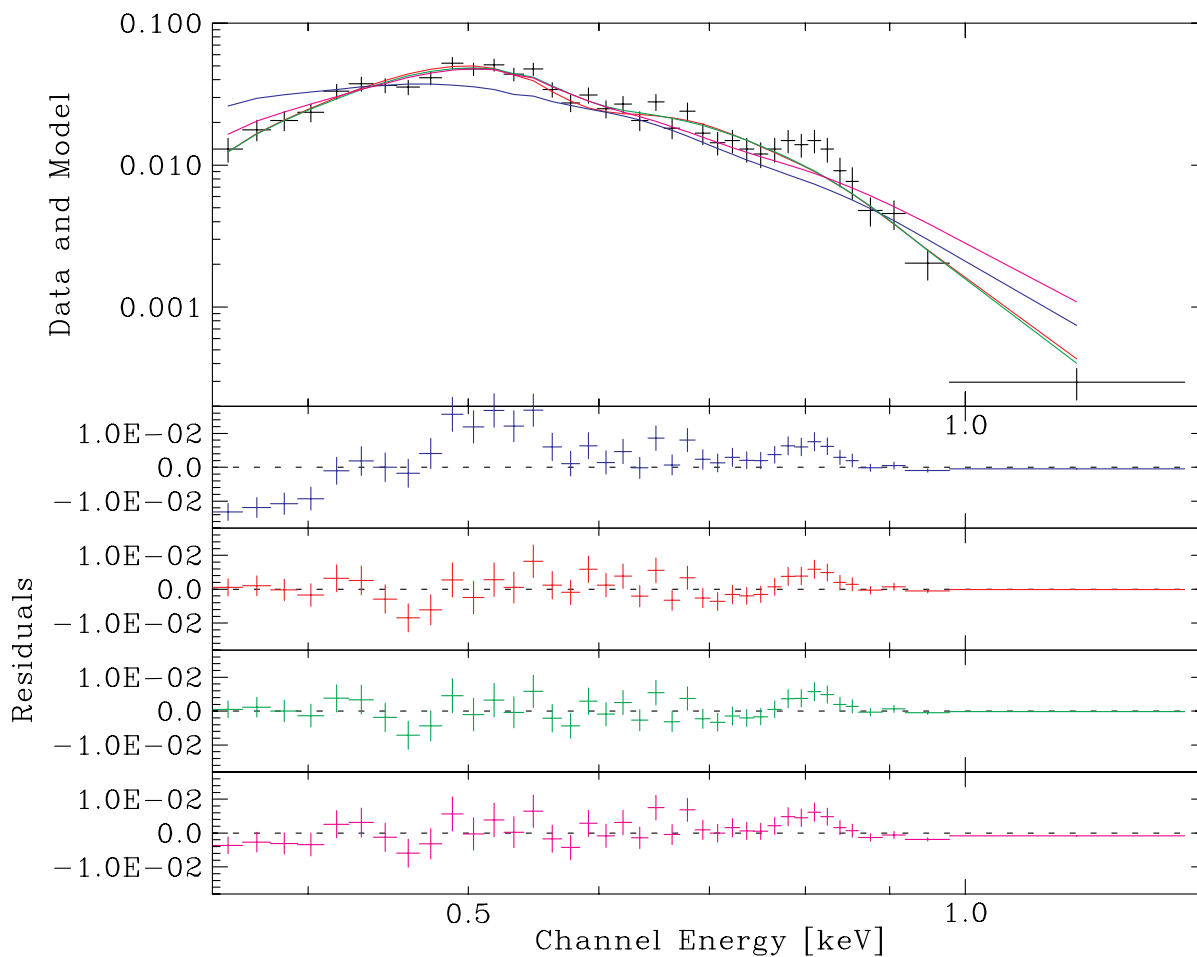


Fig. 6.— The average *Chandra* spectrum of M101 ULX-1 in 2004 July, as observed, with best-fit blackbody with a  $\xi = 1$  absorber model (blue), a blackbody with a neutral absorber model (red), a blackbody model with edges (green), and a blackbody plus diskline model (magenta). Residuals are shown for these models in the lower panels.

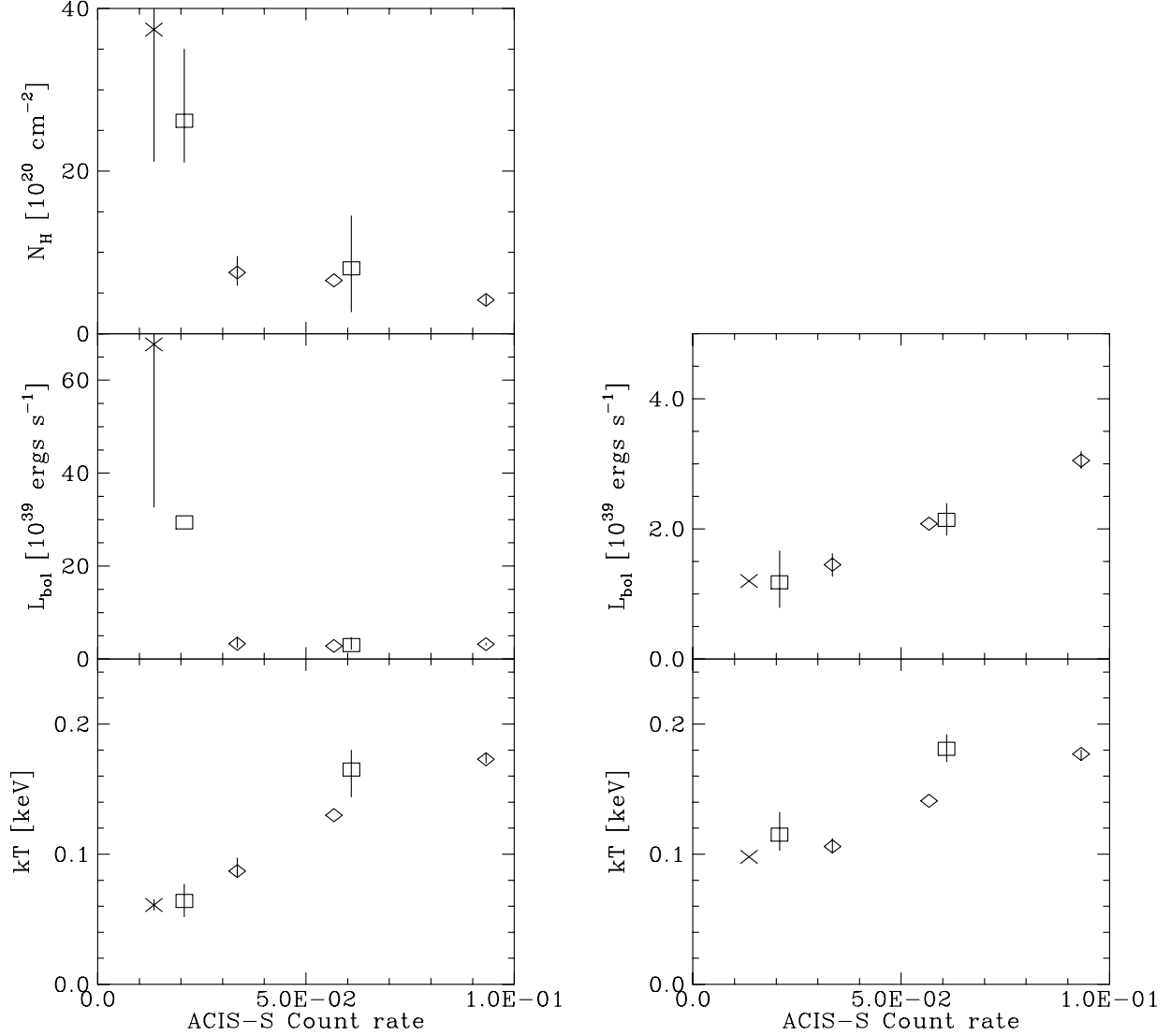


Fig. 7.— The spectral parameters plotted against scaled ACIS-S count rates using absorbed blackbody (left) and blackbody plus diskline (right) models. Symbols are diamonds for Cycle 1 data (2000 March), crosses for the combined 2004 July data, and open squares for the two Megasecond 7 pointings in 2004 December and 2005 January. For those with  $\chi^2_{\nu} < 2$ , error bars are shown, but those for  $N_{\text{H}}$  and  $L_{\text{bol}}$  for 2004 July data on the left are truncated. See text for details of the spectral models.

Table 1. X-ray Observations of M101 ULX-1.

Observatory	Observation ID	Date	MJD	Exposure (ksec) <sup>a</sup>	Notes
<i>ROSAT</i>	RP600108n00	1991-06-08	48416	33.9 ksec	PSPCB
<i>ROSAT</i>	RH600092n00	1992-01-09	48631	18.6 ksec	HRI
<i>ROSAT</i>	RH600383n00	1992-12-10	48967	32.6 ksec	HRI
<i>ROSAT</i>	RH600820n00	1996-05-14	50218	108.9 ksec	HRI
<i>ROSAT</i>	RH600820a01	1996-11-21	50409	68.9 ksec	HRI
<i>Chandra</i>	934	2000-03-26	51629	99.5 ksec	High state <sup>b</sup>
<i>Chandra</i>	2065	2000-10-29	51846	9.8 ksec	
<i>XMM-Newton</i>	0104260101	2002-06-04	52439	13.9 ksec/21.5 ksec	
<i>Chandra</i>	4731	2004-01-19	53023	57.0 ksec	
<i>Chandra</i>	5296	2004-01-21	53025	3.2 ksec	
<i>Chandra</i>	5297	2004-01-24	53028	22.0 ksec	
<i>Chandra</i>	5300	2004-03-07	53071	52.8 ksec	
<i>Chandra</i>	5309	2004-03-14	53078	71.7 ksec	
<i>Chandra</i>	4732	2004-03-19	53083	70.7 ksec	
<i>Chandra</i>	5322	2004-05-03	53128	65.5 ksec	
<i>Chandra</i>	4733	2004-05-07	53133	25.1 ksec	
<i>Chandra</i>	5323	2004-05-09	53134	43.2 ksec	
<i>Chandra</i>	5337	2004-07-05	53191	10.1 ksec	High state <sup>b</sup>
<i>Chandra</i>	5338	2004-07-06	53192	28.9 ksec	High state <sup>b</sup>
<i>Chandra</i>	5239	2004-07-07	53193	14.5 ksec	High state <sup>b</sup>
<i>Chandra</i>	5340	2004-07-08	53194	55.1 ksec	High state <sup>b</sup>
<i>Chandra</i>	4734	2004-07-11	53197	35.9 ksec	High state <sup>b</sup>
<i>XMM-Newton</i>	0164560701	2004-07-23	53210	15.1 ksec/21.5 ksec	
<i>Chandra</i>	6114	2004-09-05	53254	67.1 ksec	
<i>Chandra</i>	6115	2004-09-08	53257	36.2 ksec	
<i>Chandra</i>	6118	2004-09-11	53260	11.6 ksec	
<i>Chandra</i>	4735	2004-09-12	53261	29.2 ksec	
<i>Chandra</i>	4736	2004-11-01	53311	78.3 ksec	
<i>Chandra</i>	6152	2004-11-07	53316	44.7 ksec	
<i>Chandra</i>	6170	2004-12-22	53361	48.6 ksec	
<i>Chandra</i>	6175	2004-12-24	53364	41.2 ksec	

Table 1—Continued

Observatory	Observation ID	Date	MJD	Exposure (ksec) <sup>a</sup>	Notes
<i>Chandra</i>	6169	2004-12-30	53369	29.8 ksec	High state <sup>b</sup>
<i>Chandra</i>	4737	2005-01-01	53372	22.1 ksec	High state <sup>b</sup>
<i>XMM-Newton</i>	0212480201	2005-01-08	53379	9.7 ksec/16.0 ksec	High state <sup>b</sup>

<sup>a</sup>For *XMM-Newton* observations, the first number is the EPIC-pn exposure time and the second is the EPIC-MOS exposure.

<sup>b</sup>Denotes observations used in our spectral analysis of the high state (there are other observations in which the source was in a high state, but did not warrant spectral analysis). All 5 sequences taken in 2004 July were combined in our analysis.

Table 2. Ionized Absorber Fit for 2004 July data.

$N_{\text{H}}$ ( $10^{21} \text{ cm}^{-2}$ )	$\xi$	kT (eV)	$\chi^2_{\nu}/\text{d.o.f}$
$3.3^{+0.7}_{-0.5}$	0.0 ( $< 10^{-4}$ )	$62.4^{+2.0}_{-5.9}$	1.3/35
1.4 <sup>a</sup>	1.0 (fixed)	89.6 <sup>a</sup>	5.7/36

<sup>a</sup>Errors not calculated because of the poorness of the fit.

Table 3. Absorbed Blackbody vs. Blackbody plus Disk Line Fits.

Data	Absorbed Blackbody Fit				Blackbody plus Disk Line Fit				
	$\chi^2_\nu$	$N_H$ <sup>a</sup>	kT (eV)	$L_{bol}$ <sup>b</sup>	$\chi^2_\nu$	kT (eV)	Line <sup>c</sup>	$L_{bol}$ <sup>d</sup>	Eq.W (eV)
2000 Mar Low	1.97	7.5	89.6	3.3	1.71	106.3	3.72	1.45	102
2000 Mar Medium	2.60	6.6	129.9	2.8	3.08	140.9	1.39	2.08	24
2000 Mar High	1.59	4.2	173.1	3.2	1.55	177.1	1.32	3.05	18
2004 Jul	1.15	32.8	61.2	67.7	1.63	98.18	3.56	1.20	125
2004 Dec	0.65	37.4	64.3	29.4	1.08	115.0	5.16	1.18	164
2005 Jan	0.80	8.0	161.8	3.0	0.77	181.1	2.65	2.14	53
2005 Jan XMM	1.85	25.6	54.74	55.8	1.36	65.26	3.63	2.25	212

<sup>a</sup>Fitted column density in  $10^{20} \text{ cm}^{-2}$ .

<sup>b</sup>Inferred bolometric luminosity of the blackbody in  $10^{39} \text{ ergs s}^{-1}$ .

<sup>c</sup>Fitted line flux in  $10^{-5} \text{ photons cm}^{-2}\text{s}^{-1}$

<sup>b</sup>Inferred bolometric luminosity of the blackbody plus that of the line in  $10^{39} \text{ ergs s}^{-1}$ .